JOURNAL OF MATERIALS SCIENCE 21 (1986) 887–894

A study of the crystallization process of $Na_{1.6}Zn_{0.8}Si_{1.2}O_4$ glass and the ionic conductivity properties of partially crystallized samples

JEKABS GRINS
Department of Inorganic Chemistry, Arrhenius Laboratory, University of Stockholm, S-106 91 Stockholm, Sweden

The crystallization process of $Na_{1.6}Zn_{0.8}Si_{1.2}O_4$ glass was studied by means of differential scanning calorimetry, X-ray powder diffraction and the platinum/carbon replication technique. Partially crystallized samples were made by rapidly cooling samples from elevated temperatures using the DSC apparatus, and the ionic conductivity of the materials was determined by means of impedance measurements conducted at lower temperatures where the crystallization rate was negligible. The glass was found to crystallize at 830 K by precipitation and three-dimensional grain-growth of a crystobalite-type phase with the same composition as the glass. The overall activation energy for the crystallization process was determined from isothermal DSC measurements to be 340 kJ mol^{-1}. The bulk ionic conductivity for partially crystallized samples increases smoothly from $9.3 \times 10^{-5}(\Omega\,cm)^{-1}$ at 600 K for the glass to $2.4 \times 10^{-3}(\Omega\,cm)^{-1}$ for the crystallized material.

1. Introduction

Increased ionic conductivities are observed in heterogeneous systems where the solid electrolyte contains a dispersed second phase (DSES = dispersed solid electrolyte systems) [1]. A dispersion of small ($\leqslant 1\,\mu m$) particles in a matrix alters the transport properties of the matrix and increases the total conductivity of the sample. Usually the dispersed phase is non-conducting, e.g. Al_2O_3 or SiO_2, but may also be a conductor, as in mixtures of AgI and AgBr [2]. Su Fang [3] studied the variation of the conductivity with degree of crystallization on quenched samples of B_2O_3–0.7 Li_2O–0.7 LiCl and found an increase in conductivity in the initial stages of crystallization. Different models have been derived, attributing the increased conductivity to a layer of high conductivity surrounding each dispersed particle. The layer is assumed to be caused by an electrical double layer at the interface of the two phases [4].

In previous studies we have investigated the solid electrolyte properties of phases in the silicate system $Na_xZn_{x/2}Si_{2-x/2}O_4$ ($2 \geqslant x \geqslant 1.25$) and the corresponding germanates [5, 6]. The best conductor was found for $x = 1.85$ in the silicate system, with $\sigma = 1.0 \times 10^{-2}(\Omega\,cm)^{-1}$ at 600 K and $E_a = 0.49$ eV. In view of the report of increased ionic conductivities in heterogeneous dispersed systems we have initiated a study of the solid electrolyte properties of glasses and partly crystallized materials in the sodium zinc silicate system defined above. The present paper thus describes the variation of the ionic conductivity with the degree of crystallinity of $Na_{1.6}Zn_{0.8}Si_{1.2}O_4$ ($x = 1.6$). The glass, prepared by the rapid solidification technique, has been characterized by its crystallization temperature and heat of crystallization. The crystallization process has been studied under both isothermal and non-isothermal conditions.

The glass and the partially crystalline material have also been investigated by means of X-ray powder diffraction and by electron microscope studies of Pt/C replicas of etched surfaces.

2. Experimental details

The glass samples were prepared by rapidly cooling melts from elevated temperatures. Appropriate amounts of dried Na_2CO_3, ZnO and SiO_2 were mixed and placed in an alumina crucible. The mixture was slowly heated in an induction furnace and held at ~ 1800 K for a few minutes. The melt was then rapidly poured on to an aluminium plate, preheated to 600 K, which was then quickly pressed together with another aluminium plate. This procedure yielded pieces of glass with ~ 1 cm^2 area and 1 mm thickness. The glass was relieved from strain by placing it in a furnace at 675 K and allowing it to cool slowly over night.

The composition was checked with an energy dispersive X-ray fluorescence attachment (Link-System) to a SEM (JEM-U3). Using the previously synthesized crystalline samples as standards, the composition was found to agree with the nominal one within the experimental error, a few atomic percent, and no impurity signal was detected.

The presence of crystalline phases in the samples was investigated by recording the powder patterns of the materials with a Guinier–Hägg focusing camera at room temperature, using Cu$K\alpha_1$ radiation and silicon as the internal standard. The powder patterns were evaluated by using a measuring system constructed at this Institute [7].

The crystallization process was studied, using

0022–2461/86 $03.00 + .12

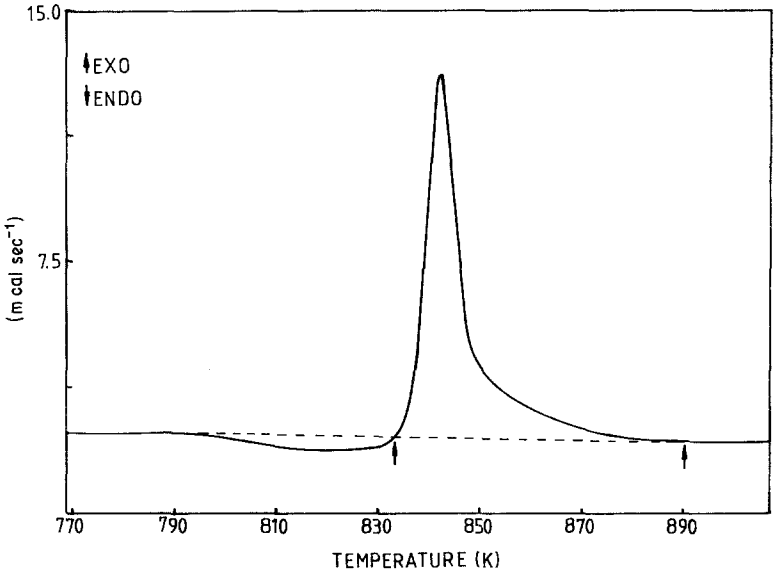

Figure 1 DSC trace recorded upon heating of non-crystallized material. Sample weight = 32.23 mg and scanning rate 10 K min^{-1}.

isothermal and non-isothermal methods, with a Perkin Elmer DSC-2 differential scanning calorimeter. The DSC apparatus was also utilized when preparing the partially crystallized samples. The temperature and heat-content readings of the instrument were calibrated, and correction was made for different scanning rates. Bulk glass pieces, 20 to 60 mg, placed in covered gold cups were used. All measurements were performed in a nitrogen atmosphere.

The partially crystallized materials were investigated with the replication technique [8]. Freshly fractured surfaces of the materials were etched with 0.1 M HNO_3 for 20 min and then vapour-coated with a mixed Pt/C layer in a single operation, using a BAE 080 Balzer high-vacuum evaporation unit with an EVM 052/EK 552 attachment. In some cases razor-blade shaped MoO_3 crystals were applied by vapourization as the test surface. The coatings were separated from the sample surfaces by immersing the specimens in dilute NaOH and they were viewed in a Philips EM 301 TEM.

The impedance measurements were made in air in the frequency range 1 Hz to 50 MHz, using a fully automated measuring system designed at this laboratory [9]. The samples were in the form of rectangular plates with 1 mm thickness and 4 to 5 mm^2 area. Blocking electrodes were applied by painting colloidal graphite onto the planar surfaces.

3. Results

3.1. Thermal analysis

A typical non-isothermal run is shown in Fig. 1. With a heating rate of 10 K min^{-1} an exothermic peak is observed at a temperature of 830 K. The peak corresponds to the transition from a glass to crystalline phase, as evidenced by X-ray powder diffraction recordings. The enthalpy change observed is 76 ± 3 J g^{-1}. About thirty degrees below the exothermic peak there is a downward shift of the baseline. This is interpreted as a glass transition. The position of the glass temperature, T_g, relative to the position of the exothermic peak did not change with the heating rate.

The variation of the peak maximum position with heating rate is often used to extract kinetic information from non-isothermal recordings [10]. Fig. 2 shows a Kissinger plot, where $\ln (Q/T_P^2)$ is plotted against $1/T_P$ (Q is the heating rate and T_P the peak maximum temperature). The slope of the straight line equals E/R where R is the gas constant and E the effective activation energy corresponding to the overall crystallization process. A least-squares fit of the data yielded an activation energy of 420 kJ mol^{-1}.

For isothermal measurements the glass samples were held at 750 K and then brought to the desired constant temperature heating at a rate of 320 K min^{-1}. Fig. 3 shows a typical isothermal recording. The measurements were analysed according to the Johnson–Mehl–Avrami (JMA) equation $\alpha = 1 - \exp(-kt^n)$ [10], assuming that the fraction of transformed material is proportional to the fractional enthalpy change (α is the fraction of material crystallized at a time t, n is a dimensionless quantity called the Avrami exponent which is numerically determined by the crystallization mechanism and k is the reaction rate constant). A rearrangement of the JMA equation

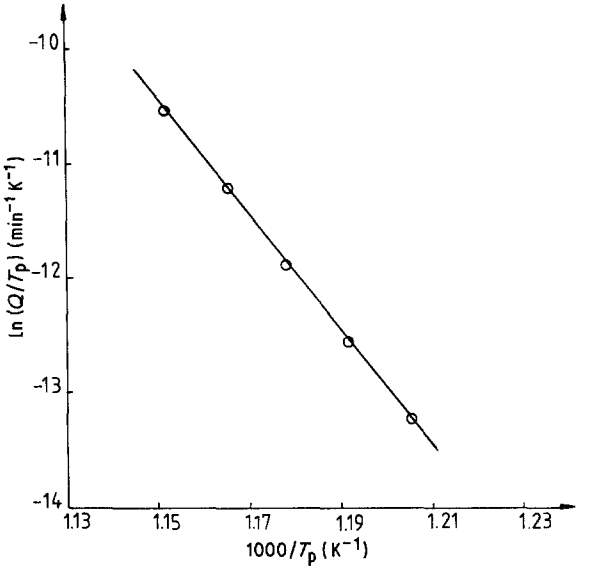

Figure 2 Kissinger plot of $\ln (Q/T_P^2)$ against $1/T_P$ for scanning rates 20, 10, 5, 2.5 and 1.25 K min^{-1}.

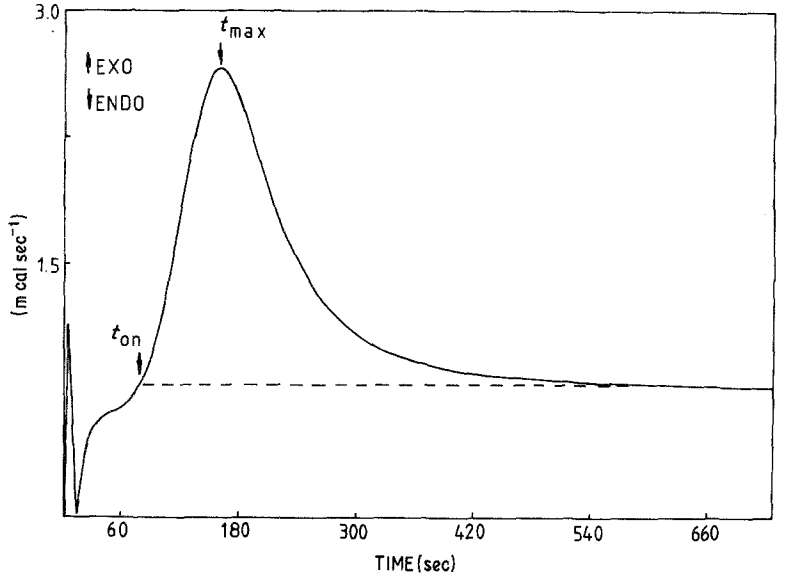

Figure 3 Typical DSC trace for isothermal crystallization of $Na_{1.6}Zn_{0.8}Si_{1.2}O_4$ glass. Sample weight = 16.61 mg and isothermal temperature 830 K. The rapid reflections of the beginning of the DSC trace derived from the time for the DSC apparatus to equilibrate.

gives $\ln[-\ln(1-\alpha)] = \ln(k) + n \ln(t)$. If the left hand side of the expression is plotted against $\ln(t)$ a straight line is obtained with a slope equal to n and an intercept equal to $\ln(k)$. Fig. 4 shows such a plot (an Avrami plot) for various isothermal temperatures.

A breakpoint is observed in the plots at a point corresponding to $\alpha = 0.4$ to 0.6. An average value of n for the first part of the plot is 2.2 ± 0.1 and for the second part 1.5 ± 0.2. No variation of n with isothermal temperature was observed. The k values used below were calculated from the first part of the plot.

The temperature dependence of k is commonly described by an Arrhenius expression $k = \nu \exp(-E/RT)$ (ν is a frequency factor, E the overall activation energy and T the absolute temperature). Fig. 5 shows a plot of $\ln(k)$ against $1/T$ for the experimental data. The slope of the straight line gives an activation energy $E = 342\,\text{kJ mol}^{-1}$.

The isothermal DSC curves exhibited an incubation period, defined as the time elapsed from the start of the isothermal run to the beginning of the transition peak, which varied with the annealing temperature. The logarithm of the time elapsed until the onset of the peak, t_{on} (see Fig. 3), and the logarithm of the time elapsed until peak maximum, t_{max}, are plotted against the reciprocal of the annealing temperature in Fig. 6. In both cases straight lines were obtained, indicating an Arrhenius type of behaviour with an activation energy of $333\,\text{kJ mol}^{-1}$.

It can also be noted that isothermal runs, made on samples which had been preheated by a non-isothermal DSC run up to the very onset of the exothermal peak, did not exhibit any incubation period. This indicates that nucleation centres are formed prior to the main crystallization process.

Both isothermal and non-isothermal runs were made on material which had been crushed to powder. No significant change in onset temperatures or transition enthalpies could be observed. This is interpreted as evidence for bulk crystallization that is not initialized at the surface of the material.

The partly crystallized samples used in the replication, X-ray and impedance studies described below were prepared by interrupting non-isothermal heating

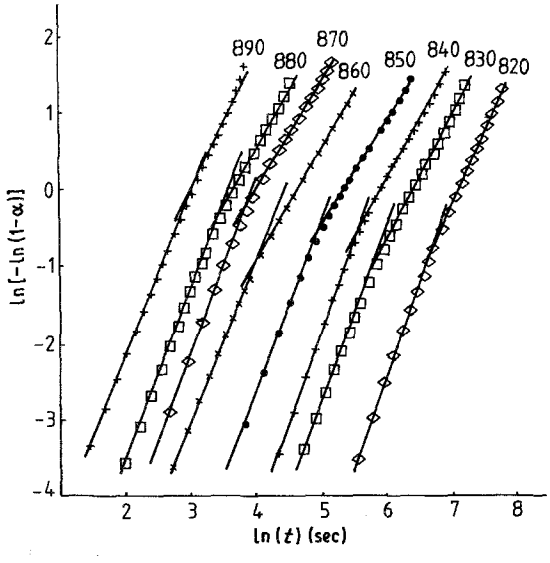

Figure 4 JMA plots of $\ln[-\ln(1-\alpha)]$ against $\ln(t)$ for isothermal crystallization of $Na_{1.6}Zn_{0.8}Si_{1.2}O_4$ glass at various annealing temperatures 820 to 890 K.

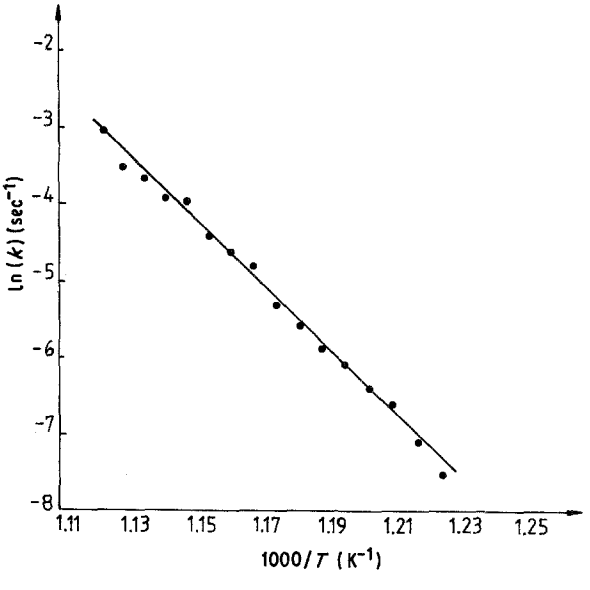

Figure 5 $\ln(k)$ plotted against the inverse of the annealing temperature.

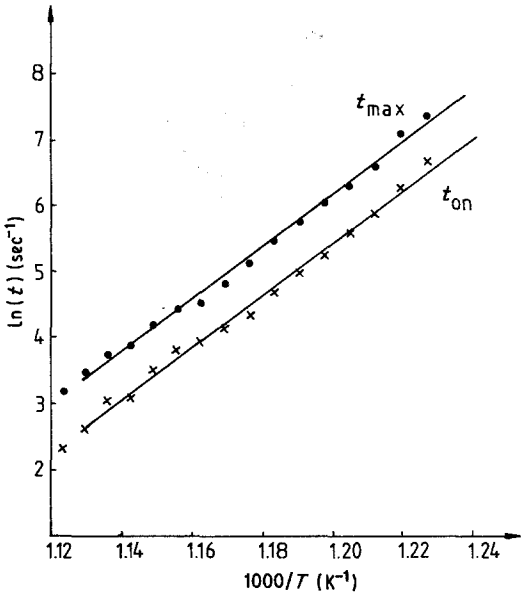

Figure 6 The logarithm of the time elapsed from the beginning of the annealing experiment to the onset of the peak, t_{on}, and to the peak maximum, t_{max}, in the isothermal measurements, plotted against the inverse of the annealing temperature.

runs at appropriate temperatures, as monitored by the DSC-trace. The samples were then quenched to room temperature in the DSC-equipment at a rate of $\sim 300\ K\ min^{-1}$.

The fraction of crystallized material in the partly crystallized samples, α, was estimated from the fraction of the total transition ehthalpy observed at the point of interruption. The feasibility of halting the crystallization process was checked by re-running a number of quick-cooled samples in a second heating. The transition enthalpy then observed agreed with the estimated remaining fraction of the transition enthalpy.

3.2. X-ray diffraction

The X-ray powder photograph of partially crystallized samples showed that only one phase precipitated during the crystallization. This phase was found to be identical with the one observed for compositions close to $Na_{1.6}Zn_{0.8}Si_{1.2}O_4$ in the previous study of the sodium–zinc–silicate system [5]. All reflections but one could be indexed on the basis of a cubic unit cell with $a = 0.7316 \pm 0.1$ nm. The lattice parameter did not change with the degree of crystallization.

The previous study showed that this phase decomposed into a mixture of two phases upon prolonged heat treatment below 1025 K. The disintegration rate was, however, observed to be small, explaining the absence of evidence for such behaviour in the present study.

3.3. Replication studies

A replica from a non-crystallized sample is shown in Fig. 7. The replica shows an even surface with some structure at a level of 10.0 nm. A flat MoO_3 crystal is seen in the upper part of the micrograph.

Samples rapidly cooled after heating above the glass transition temperature but below the onset of the crystallization, as monitored by the DSC trace, gave replicas of the type shown in Fig. 8. Scattered aggregates of granules with diameters ~ 50.0 nm are observed on an otherwise smooth surface. The granules are interpreted as consisting of prematurely crystallized material. Such precipitation may have occurred near strains of compositional inhomogeneities.

A representative replica from a partially crystallized sample is shown in Fig. 9. The transformed fraction, α, of the sample is estimated to be ~ 0.2. A granulated surface is observed with the granule size ~ 50 to 100 nm. The small crystallite size and the fact that the glass and crystalline phase are of the same composition lessen the visualizing effect of the etching. Similar replicas were obtained from samples with other α values. The replicas from materials with higher α values showed a rougher surface with more clearly protruding crystallites, which illustrates the decreasing amount of amorphous material with increasing α

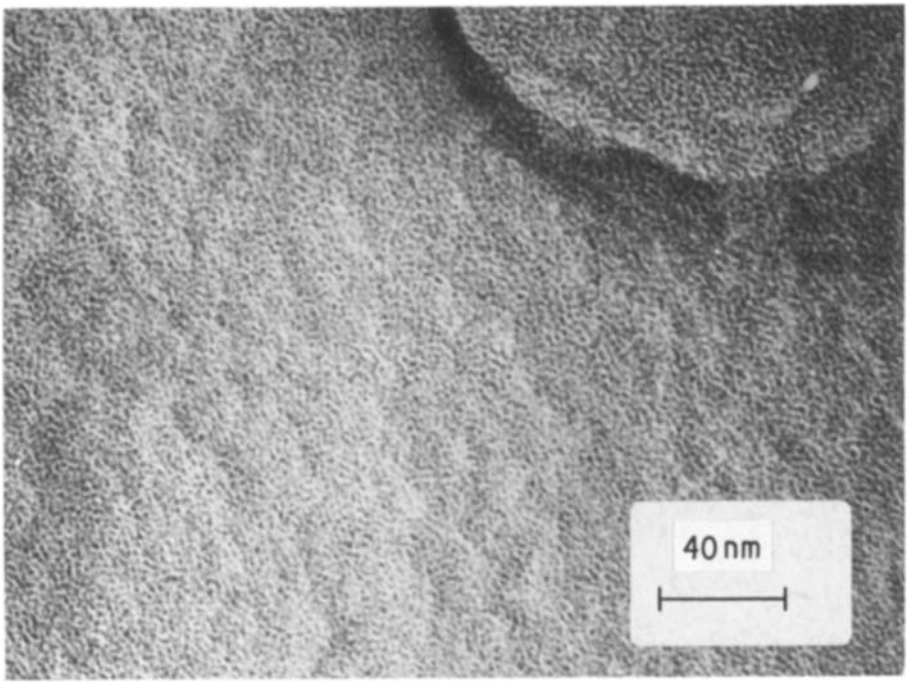

Figure 7 A replication electron micrograph of a non-crystallized sample. An MoO_3 crystal is seen in the upper left corner.

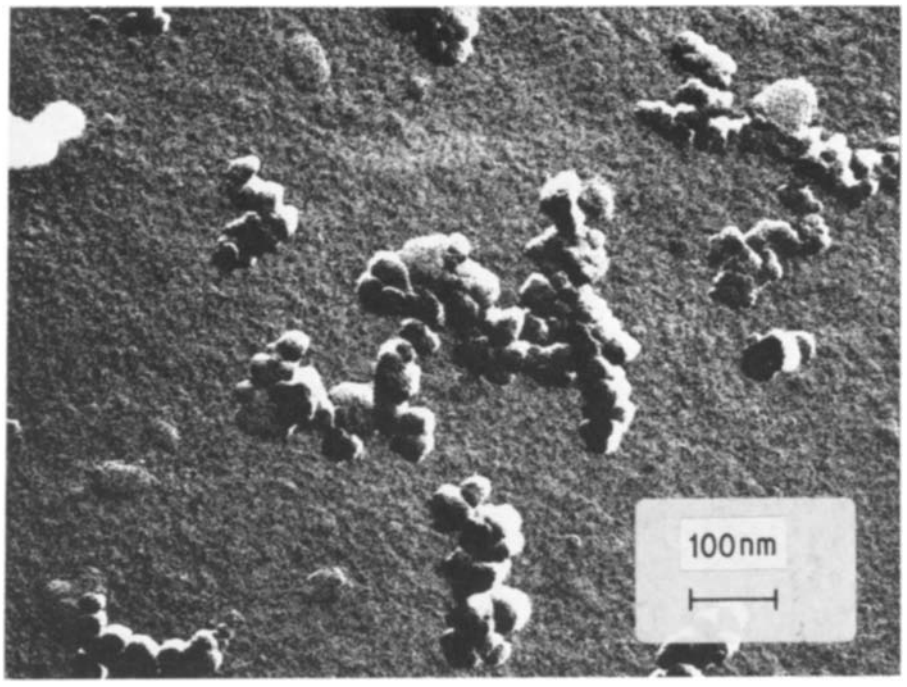

Figure 8 A replication electron micrograph of a sample from a DSC heating run interrupted at a temperature between the glass temperature and the onset of the crystallization.

values. No other difference in appearance could be observed between samples with α values larger and smaller than 0.4 to 0.6, where the breakpoints were found in the Avrami plots.

Samples annealed at 925 K for about 3 h became milky, almost opaque in appearance. A replica of an annealed sample is shown in Fig. 10. A characteristic, clearly visible, surface structure is observed, interpreted as consisting of crystalline grains with a size of 60 to 300 nm, separated by grain boundaries.

3.4. Impedance measurements

The impedance was measured as a function of frequency at an average of nine temperatures per sample for samples with different fractions of crystalline material. For each temperature the impedance was plotted in the complex impedance plane and the ionic conductivity determined from the intersection of the semi-circle with the real axis. Most of the samples yielded only one semi-circle in the complex impedance plane, but a few samples produced an additional one, apparently not connected with the electrode processes. An example of an impedance plot showing two semi-circles is given in Fig. 11. The first circle was in all cases symmetrical, with the centre positioned close to the real axis. Within the frequency range of this first circle there was no substantial frequency dependence of the conductivity or permittivity. The activation energies, E_a, and pre-exponential factors, $\log(\sigma_0)$, were calculated by fitting the data to the equation $\ln(\sigma T) = \ln(\sigma_0) - E_a/kT$, and they are listed in Table I together with values of $\log(\sigma T)$ at $T = 600$ K. Conductivity parameters designated by (1) were calculated from the first non-zero intercept, those designated by (tot) from the second intercept and those by (2) from the value of the second intercept

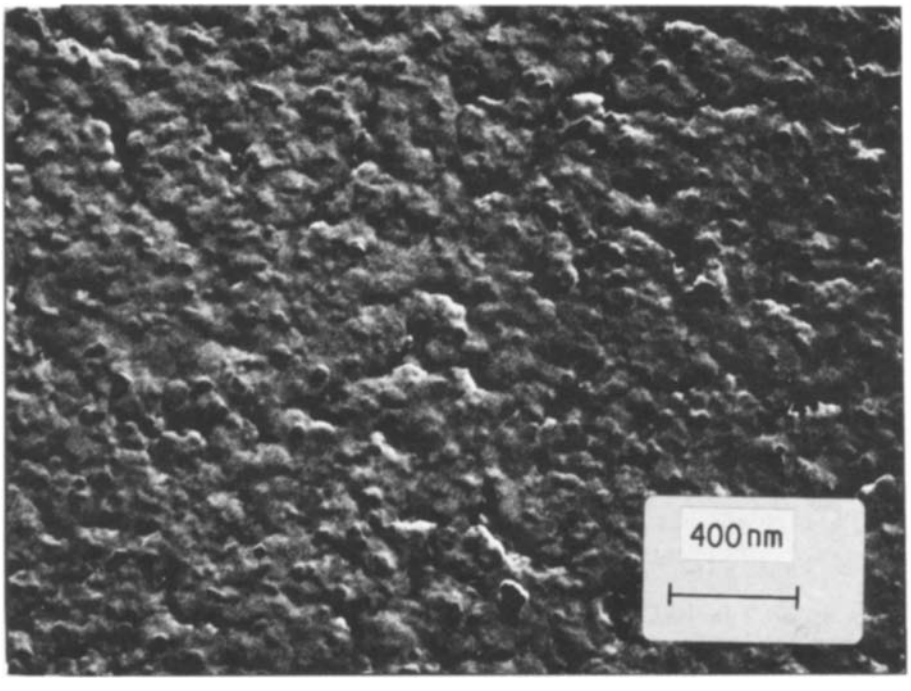

Figure 9 A replication electron micrograph of a partially crystallized sample. The transformed fraction is estimated to be ~0.2. Magnification × 22 000.

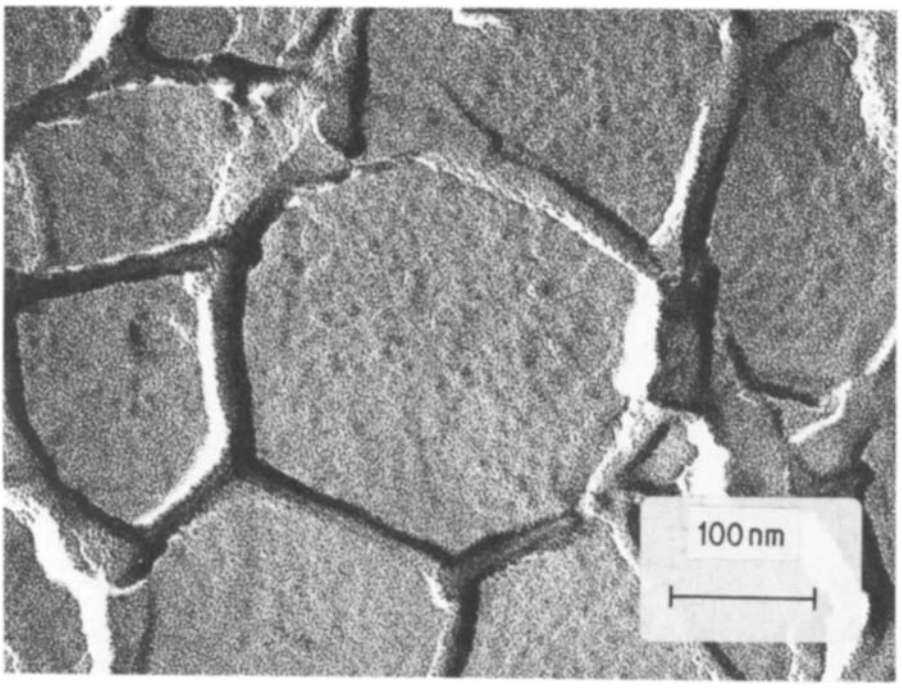

Figure 10 A replication electron micrograph of sample, heat-treated at 925 K for 3 h. Magnification × 98 000.

minus the value of the first. The same bulk geometric factor was used in all three cases. The statistical errors are estimated as ± 0.005 eV in E_a and ± 0.1 in log (σ_0) for the designations (1) and (tot) but are much higher for (2), especially when the semi-circles overlap substantially. The samples designed by B in the table were quick-cooled from increasing temperatures above the glass transition, T_g, but below the exothermic crystallization peak and those designated by A from temperatures within the larger exothermic peak. The α values were estimated from the DSC recordings.

The samples exhibiting a second circle were mainly those from the later stages of crystallization, 16, and the annealed sample, 17. One sample, 11, with an estimated α value of 0.25 also exhibited a small second semi-circle.

No systematic variation of the conductivity parameters was observed for samples within the B series; this is interpreted as being characteristic of the glass phase. Averaging produces $E_a = 0.721 \pm 0.003$ eV, log $(\sigma_0) = 4.80 \pm 0.08\,(\Omega\,\mathrm{cm})^{-1}$ and log (σT) at $T = 600\,\mathrm{K} - 1.253 \pm 0.075\,(\Omega\,\mathrm{cm\,K^{-1}})^{-1}$. The crystallized samples yield two semi-circles in the complex impedance plane. The intersection of the first semi-circle with the real axis gives a good estimate of the conductivity parameters of the crystalline phase. The obtained values are $E_a = 0.640 \pm 0.006$ eV, log $(\sigma_0) = 5.58 \pm 0.16\,(\Omega\,\mathrm{cm})^{-1}$ and log (σT) at 600 K $0.17 \pm 0.15\,(\Omega\,\mathrm{cm\,K^{-1}})^{-1}$. The conductivity of the crystalline phase is thus ~ 30 times higher than the conductivity of the glass phase at 600 K.

The change in activation energy, pre-exponential

TABLE I Conductivity data for partially crystallized $Na_{1.6}Zn_{0.8}Si_{1.2}O_4$ samples

Sample number	E_a (eV)	log (σ_0) $(\Omega\,\mathrm{cm})^{-1}$	log (σT) at 600 K $(\Omega\,\mathrm{cm\,K^{-1}})^{-1}$	Fraction crystallized material, α	
1	0.748	5.10	−1.198	0	Not heated in the DSC
2 B	0.719	4.68	−1.355	0	B; rapidly cooled from temperatures
3 B	0.717	4.75	−1.285	0	between the glass temperature
4 B	0.719	4.91	−1.140	0	and the onset of the exothermal
5 B	0.726	4.77	−1.328	0	peak
6 B	0.723	4.85	−1.226	0	
7 B	0.723	4.83	−1.230	0	
8 B	0.720	4.82	−1.215	0	
9 A	0.721	4.84	−1.205	0.05	A; rapidly cooled from within the
10 A	0.718	4.99	−1.033	0.1	larger exothermal peak
11 A(1)	0.668	5.18	−0.445	0.25	
(2)	0.86	8.4	–		Large errors in conductivity
(tot)	0.691	5.38	−0.445		parameters for 2nd circle
12 A	0.676	5.13	−0.594	0.3	
13 A	0.682	5.25	−0.508	0.35	
14 A	0.683	5.32	−0.419	0.5	
15 A	0.640	5.37	−0.052	0.75	
16 A(1)	0.646	5.59	+0.133	1.0	The conductivity does not exhibit
(2)	0.419	4.24	+0.732		Arrhenius behaviour for 2nd
(tot)	0.621	5.29	+0.038		circle
17 (1)	0.642	5.74	+0.300	1.0	Annealed at 925 K for 3 h, nearly
(2)	0.430	3.69	+0.193		opaque samples
(tot)	0.567	4.70	−0.058		

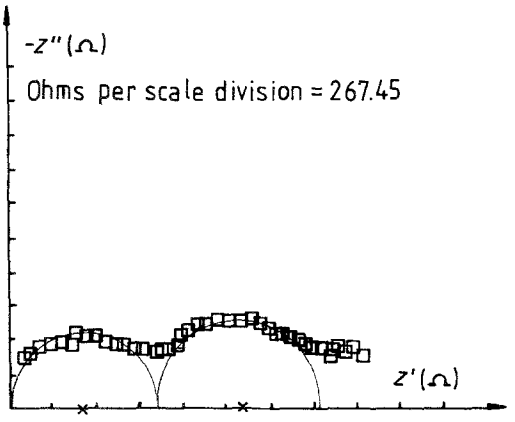

Figure 11 Complex impedance plot ($Z = Z' + iZ''$) for a complete crystallized sample (No. 17) of $T = 541$ K.

factor and conductivity at 600 K with increasing crystallinity is shown in Fig. 12, where the conductivity parameters are plotted against the estimated fraction α of crystalline phase. As far as can be judged the conductivity increases smoothly with α.

4. Discussion

The replication studies show that the grain-growth during the crystallization process is three-dimensional. The grains in the fully crystallized samples are small (~ 0.05 to $0.2\,\mu$m) and the samples visually transparent. This indicates a very rapid nucleation.

Replication electron micrographs of materials heated to a temperature between the glass temperature and the crystallization temperature show clusters of crystallites (Fig. 8). The occurrence of such crystallites explains why these samples did not show any incubation period upon subsequent isothermal treatment, as mentioned above. The spherical appearance of the crystallites indicates a three-dimensional growth, which would give an n-value in the Avrami plots of 3 or 4 in the case of growth limited by interface advance, depending on whether nucleation is "instantaneous" or constant-rate. The shape of the non-isothermal crystallization DSC peak and the formation of crystallites within the glass transition region suggest that these two processes partly overlap. Such an overlap might produce an n-value of 2.2 rather than the expected value of 3. The crystallite clusters might also serve as heterogeneous nucleation sites upon further crystallization. In the case of such a heterogeneous nucleation, the JMA treatment would not be valid.

The activation energies for the crystallization process, obtained from isothermal and non-isothermal DSC runs, were 342 and 420 kJ mol^{-1}, respectively. Following Yinnon and Uhlman [10], the overall activation energy can be written as $E \cong (E_N + mE_G)/n$ for a constant rate nucleation and $E \cong E_G$ if the nucleation is instantaneous (E_N and E_G are the effective activation energies for nucleation and grain-growth respectively, n is the Avrami exponent and m a constant determined by the growth mechanism and is 1, 2 or 3 for one-, two- or three-dimensional interface-advance growth). The difference in activation energy values might be due to a difference in nucleation rate between the two sets of measurements. Assuming that in the non-isothermal DSC runs the nucleation is instantaneous, the first case described above would be valid and give $E = 420\,\text{kJ mol}^{-1} \cong E_G$. In isothermal runs the nucleation rate might be

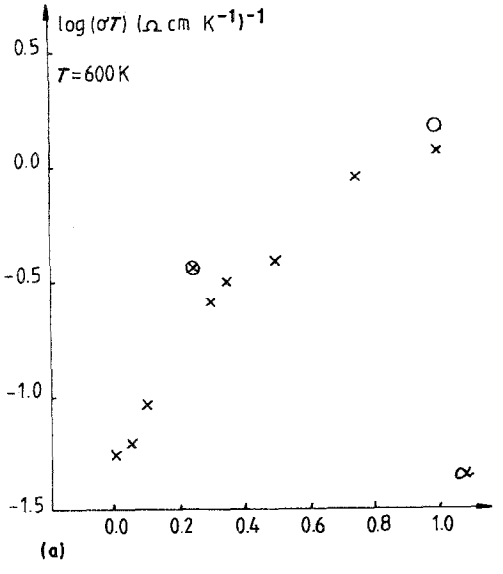

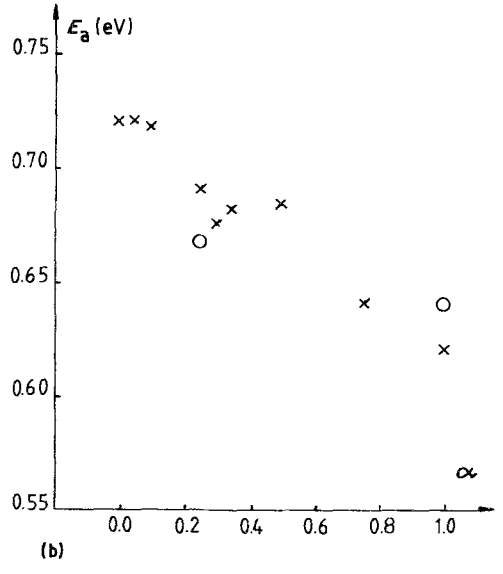

Figure 12 The conductivity parameters (a) E_a, (b) log (σ_0) and (c) log (σT) at 600 K plotted against the fraction α of crystallized material in the samples. (x, 0 = conductivity parameters denoted by tot and 1, respectively in Table I and text.)

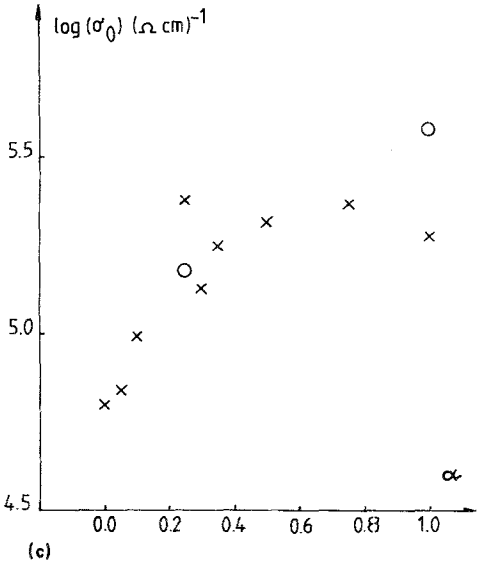

low enough to allow a simultaneous grain growth. If one assumes $E_N \ll E_G$, $m = 3$ and $n = 4$, a constant-rate nucleation would give $E \cong (3/4)E_G = 315\,\text{kJ mol}^{-1}$, compared with the experimentally obtained $342\,\text{kJ mol}^{-1}$.

This possibility is apparently substantiated by measurements which were performed on samples that were not relieved of strain. These measurements yielded closely agreeing activation energy values of 458 and $454\,\text{kJ mol}^{-1}$ for isothermal and non-isothermal runs, respectively. The higher activation energy obtained for samples not relieved of strain in isothermal runs might, accordingly be due to a higher nucleation rate in these samples, caused by the strain.

The frequency dependence of the conductivity and permittivity of a heterogeneous system of conducting dielectrics has been discussed by Volger [11] for the case of a stratified body and by Fricke [12], for the case of a suspension of ellipsoids.

Assuming that the dielectric constants for two conducting phases, a and b, are approximately the same, the conductivity of a stratified body of the two phases can be shown to approach a value $\sigma_{00} \cong v_a\sigma_a + v_b\sigma_b$ at high enough frequencies (v_a and v_b are the volume fractions of the two phases. If $\sigma_a \ll \sigma_b$ the expression simplifies further to $\sigma_{00} \cong v_a\sigma_a$). At low frequencies another conductivity limit is found; $\sigma_s = \sigma_a\sigma_b/(v_b\sigma_a + v_a\sigma_b)$.

The conductivities in Table I were calculated from the intersections of the real axis in the complex impedance plane. Two semi-circles were observed for fully crystallized samples. The intersection with the first semi-circle is interpreted as corresponding to the conductivity of the crystalline phase. The second intersection is interpreted as corresponding to the resistance of either grain-boundaries or, possibly, since the precipitated phase is meta-stable, the resistance of small amounts of another phase or phases between grains. The origin of the observed small second semi-circle for sample 11 with $x \cong 0.25$ is ambiguous.

With the exception of sample 11, the partly crystallized samples showed only one semi-circle. The conductivities of these samples could thus not be separated into components corresponding to the glass and crystalline phases. A small frequency dependence of the conductivities and permittivities was observed. A frequency-dependent conductivity can, however, be interpreted as being due either to a broad transition between two, unobservable, levels, σ_s and σ_{00}, or to a general dielectric response of the kind proposed by Jonscher [13].

The conductivities do not exhibit any anomalous increase during the crystallization process, despite the small size of the precipitated crystallites, which should promote such an effect. The reason for this is not clear. One possible explanation is that the dispersed phase must differ sufficiently in composition from the matrix to generate the electrical double layer which is responsible for the conductivity increase. Another possibility is that, if the increased conductivities in disperse systems of e.g. silver halides are due to an increase of the concentration of defects (e.g. interstitial Ag^+ ions), then it might be that the conduction mechanism in the materials investigated here is not dependent on the existence of such defects.

Acknowledgement

The author is pleased to thank Dr M. Nygren for his great interest in this study and for many fruitful discussions. This work has been financially supported by the Swedish Natural Science Research Council.

References

1. J. B. WAGNER Jr, *Mater. Res. Bull.* **15** (1980) 1091.
2. K. SHAHI and J. B. WAGNER, *Solid State Ionics* **3/4** (1981) 295.
3. SU FANG, *ibid.* **7** (1982) 37.
4. J. MAIER, in "Reactivity of Solids" (Materials Science Monographs 28a), edited by P. Barret and L.-C. Dufour (Elsevier, 1985) p. 417.
5. J. GRINS, *Solid State Ionics* **7** (1982) 157.
6. J. GRINS and M. NYGREN, *ibid.* **9/10** (1983) 864.
7. K.-E. JOHANSSON, T. PALM and P.-E. WERNER, *J. Phys. E* **13** (1980) 128.
8. W. VOGEL, L. HORN, H. REISS and G. VÖLKSCH, *J. Non-Cryst. Solids* **49** (1982) 221.
9. T. HÖRLIN, *Chem. Scripta* in press.
10. H. YINNON and D. R. UHLMAN, *J. Non-Cryst. Solids* **54** (1982) 253.
11. J. VOLGER, *Progr. Semicond.* **4** (1960) 207.
12. H. FRICKE, *J. Phys. Chem.* **57** (1953) 934.
13. A. K. JONSCHER, *Phys. Status Solidi (a)* **32** (1975) 665.

Received 11 February
and accepted 21 May 1985